Chemical Geology 547 (2020) 119662

Contents lists available at ScienceDirect

Chemical Geology

journal homepage: www.elsevier.com/locate/chemgeo

A new purification method for Ni and Cu stable isotopes in seawater provides evidence for widespread Ni isotope fractionation by phytoplankton in the North Pacific

Shun-Chung Yang[a,*], Nicholas J. Hawco[a,b,**], Paulina Pinedo-González[c], Xiaopeng Bian[a], Kuo-Fang Huang[d], Ruifeng Zhang[e], Seth G. John[a]

[a] Department of Earth Sciences, University of Southern California, Los Angeles, CA, USA
[b] Department of Oceanography, University of Hawai'i at Manoa, Honolulu, HI, USA
[c] Lamont Doherty Earth Observatory, Columbia University, Palisades, NY, USA
[d] Institute of Earth Sciences, Academia Sinica, Taipei, Taiwan
[e] School of Oceanography, Shanghai Jiao Tong University, Shanghai, China

ARTICLE INFO

Editor: Oleg Pokrovsky

Keywords:
δ^{60}Ni
δ^{65}Cu
Chromatography
Trace metal cycling
Phytoplankton

ABSTRACT

Nickel and copper are cofactors in key phytoplankton enzymes and the stable isotope composition of Ni and Cu (δ^{60}Ni and δ^{65}Cu) in seawater have the potential to identify major processes that influence their biogeochemistry. However, accurate analysis of δ^{60}Ni and δ^{65}Cu is challenging because of the difficulties in separating these metals from interfering elements in the seawater matrix. Here we report a fast and simple method for purification of Ni and Cu from seawater samples that is able to completely remove interfering elements Mn, Ti, Cr, and Fe. This method was verified by analyzing four reference materials that contain significant levels of interfering elements (powdered plankton, natural soils, and two marine sediments). Using this technique, we generated a dataset of 49 seawater δ^{60}Ni and δ^{65}Cu measurements from the upper water column of the North Pacific Ocean, which show preferential uptake of light Ni isotopes by phytoplankton ($\alpha_{bio\text{-}sw}$ = 0.9997 ± 1) but no net fractionation of Cu isotopes. This new method simplifies treatment of seawater samples for Ni and Cu isotope analysis, enabling high-throughput investigations of δ^{60}Ni and δ^{65}Cu throughout the global ocean.

1. Introduction

Many aspects of the marine biogeochemistry of nickel (Ni) and copper (Cu) are unresolved. Both metals are nutrients to phytoplankton, but are not fully depleted in the surface ocean (Boyle et al., 1981; Moore et al., 2013). Both elements are regenerated in the water column, but are decoupled from major nutrients like phosphorus (Bruland, 1980; Boyle et al., 1977). Relative to other divalent metals, Ni and Cu also form the strongest complexes with organic ligands (Irving and Williams, 1953), but whereas most Ni is found in labile, presumably inorganic, species (Achterberg and Van Den Berg, 1997; Saito et al., 2004, 2005; Boiteau et al., 2016), Cu is almost completely bound by strong organic ligands (Coale and Bruland, 1990; Jacquot and Moffett, 2015; Whitby et al., 2018). Because of their strong binding, both metals may be toxic under certain conditions, often because they outcompete other metals for protein binding sites (Sunda and Huntsman, 1998; Macomber and Imlay, 2009; Hawco and Saito, 2018). As a result, efflux pumps and sensor proteins for Cu and Ni are widespread (Waldron and Robinson, 2009; Huertas et al., 2014). It remains to be seen whether the scarcity or toxicity of Ni and Cu affect phytoplankton growth in the oceans.

Over the past two decades, ion chromatography and multi-collector ICP-MS techniques have been developed to measure Ni and Cu isotopes in seawater (Bermin et al., 2006; Cameron et al., 2009; Takano et al., 2017), which has raised additional questions about their biogeochemistry. Initial reports highlighted somewhat homogenous profiles of δ^{65}Cu and δ^{60}Ni, despite significant concentrations gradients between surface and deep waters (Vance et al., 2008; Cameron and Vance, 2014). The heavy δ^{60}Ni and δ^{65}Cu composition of the oceans compared to crustal material – roughly +1.4‰ and +0.65‰, respectively – has also emphasized the lack of isotope mass balance in the marine Ni and Cu cycles, suggesting the existence of unidentified sources or sinks of

* Corresponding author.
** Correspondence to: N.J. Hawco, Department of Oceanography, University of Hawai'i at Manoa, Honolulu, HI, USA.
E-mail addresses: shunchuy@usc.eduv (S.-C. Yang), hawco@hawaii.edu (N.J. Hawco).

https://doi.org/10.1016/j.chemgeo.2020.119662
Received 25 November 2019; Received in revised form 4 May 2020; Accepted 6 May 2020
Available online 16 May 2020
0009-2541/

these metals (Vance et al., 2016; Ciscato et al., 2018; Little et al., 2014, 2017).

More recently, deviations from mean ocean δ^{65}Cu and δ^{60}Ni have been identified. Takano et al. (2017) and Archer et al. (2020) observed δ^{60}Ni up to +1.7‰ in South Pacific and South Atlantic surface waters, suggesting biological uptake of isotopically light Ni. This conflicts with the observations of Wang et al. (2019), who found no evidence for Ni isotope fractionation during phytoplankton Ni uptake in Southern Ocean waters. Variations in δ^{65}Cu have also been observed in the upper ocean, and have been hypothesized to reflect biological uptake, Cu ligand production, or new Cu sources (Takano et al., 2014; Little et al., 2018; Baconnais et al., 2019). However, interpretation of these δ^{65}Cu observations has been complicated because of incomplete Cu extraction and insufficient replication.

The reproducibility and sample throughput of isotopic analyses have limited the generation of isotopic data from high resolution transects (e.g. GEOTRACES). Purification of Ni and Cu from seawater has proven particularly challenging. Successful purification protocols must separate Ni and Cu from other inorganic elements in the seawater matrix that may interfere the analysis of δ^{60}Ni and δ^{65}Cu, especially Na, Mg, Ca and S. The utilization of Nobias-PA1 resin, which can extract ≥99% of Ni and Cu from the seawater matrix, has partially succeeded in addressing this problem (e.g. Takano et al., 2017; Little et al., 2018). However, micro-gram levels of primary matrix elements are still present, usually at one order of magnitude higher concentrations than Ni and Cu (Takano et al., 2017). Furthermore, minor elements, including Mn, Ti, Cr and Fe can interfere with δ^{60}Ni and δ^{65}Cu measurements and also bind to Nobias-PA1 resin. Further purification is therefore necessary. Successful purification can require high quantities of AG-MP1 anion exchange resin (0.6–2 mL) and high aspect ratio columns (lengths ≥5 cm, e.g. Borrok et al., 2007; Takano et al., 2017; Wang et al., 2019), which often lead to longer purification times. Even with these modifications, it can be difficult to fully remove interfering elements without compromising Ni and Cu recovery if each column is not carefully calibrated. Non-reusable resins like Eichrom TRU Spec Resin or Nickel Resin have allowed researchers to further remove interfering elements (e.g. Archer and Vance, 2004; Cameron and Vance, 2014; Vance et al., 2016), but their cost may restrict sample throughput and may not remove all interfering elements from the matrix.

Here we describe a new purification method that quickly and effectively separates Ni and Cu from elements that interfere with ICPMS analysis, and can be coupled to existing methods to purify other metals in interest (e.g. Fe, Zn and Cd). We applied these techniques to measure δ^{60}Ni and δ^{65}Cu in 49 seawater samples, but this purification approach is also suitable for other geochemical applications. Furthermore, the simplicity of this method highlights its potential for automation by robotic sample processing systems (e.g. prepFAST), which can greatly increase the number of high quality δ^{60}Ni and δ^{65}Cu measurements that can be made.

2. Experimental

2.1. Reagents, standards, reference materials and samples

All sample preparation work was carried out in flow benches with Ultra Low Particulate Air (ULPA) filtration within a class 100 clean room at the University of Southern California. Ultrapure reagents were purchased from the manufacturer (BDH Aristar Ultra HF, HBr, HN_4OH and H_2O_2; Fluka traceSELECT methanol) or purchased in a lower grade and further purified by sub-boiling distillation in a PFA still (BDH Aristar Plus: HCl, HNO_3, and acetic acid). Ultrapure water (Milli-Q; 18.2 MΩ) was used throughout. All steps involving concentrated acids were performed in acid-cleaned PFA (Savillex), and purified sample solutions were stored in acid-cleaned polyethylene (LDPE, VWR Metal-free centrifuge tubes). All equipment was handled with polyethylene gloves. Before use, batches of Nobias-PA1 resin were cleaned in 3 M nitric acid for several days and rinsed with ultrapure water. Likewise, AG-MP1 resin was cleaned in 10% hydrochloric acid solution and stored in ultrapure water until use.

For the assessment of column elution procedures, Ni and Cu isotope ratios were measured in the reference materials including BCR-414 (European Commission; powdered and freeze-dried plankton), Arizona Test Dust (Powder Technologies Incorporated); natural soils collected in the southwestern US and sifted to include particles only in the 1–100 μm range; lot 10386BK, PACS-2 (National Research Council of Canada; marine sediments collected in the harbor of Esquimalt) and MESS-3 (National Research Council of Canada; marine sediments collected from the Beaufort Sea).

The 49 seawater samples reported in this study were collected during the Gradients expedition in the North Pacific aboard the R/V Ka'imikai-O-Kanaloa in April 2016 during a latitudinal transect along 158° W from 23°N to 38°N. Samples were collected from the upper 600 m of the water column using 8 L external-spring Niskin bottles modified for trace-metal sampling with titanium and Delrin brackets (Ocean Test Equipment) mounted on an epoxy-coated rosette and deployed on an Amsteel line. After collection, seawater was filtered through 0.2 μm Acropack cartridge filters (Pall) into acid-washed 4 L low density polyethylene bottles (Nalgene).

2.2. Sample pretreatment and preconcentration

For reference materials, approximately 100 μg of sample was digested by heating overnight on a hotplate at 120–130 °C with 1.7 mL of 14 M HNO_3, 1 mL of 11 M HCl and 1 mL 28 M HF in a 7 mL PFA vial, and then evaporated to dryness at 120–130 °C. To further decompose organic matter, samples were re-dissolved with 1 mL of 14 M HNO_3 and 1 mL of 35% H_2O_2 and heated overnight at 120–130 °C, and evaporated to dryness at 120–130 °C. Samples were then re-dissolved with 0.5 mL 0.05 M ammonium acetate buffer (pH = 6.0 ± 0.2) for Ni and Cu preconcentration with Nobias-PA1 resin. Nobias PA1 resin (0.6 mL) was loaded in Bio-Spin® Disposable Chromatography Columns (#7326008; id ~6.4 mm) and sample solution was loaded onto the resin. The resin was then rinsed with 5 mL 0.006 M ammonium acetate buffer

Table 1
Protocol for preconcentration of Ni and Cu by Nobias-PA1 resin.

For seawater	For reference material	Collection
a. Adding 2.5 mL pre-cleaned resin in seawater; shaking overnight	a. Loading 0.6 mL resin into a column, cleaning resining with 5 mL 1 M HNO3, rinse with Milli-Q water, and conditioning with 0.05 M CH_3COONH_4 (pH = 6)	
b. Adjusting sample pH to 6 with CH_3COONH_4 and HN_4OH; shaking for ~5 h	b. Loading sample onto resin (in 0.05 M CH_3COONH_4, pH = 6)	
c. Filtering resin	c. Loading sample onto resin	Na, Mg, Ca, P, S
d. Rinsing with ~125 mL Milli-Q water	d. Rinsing with 5 mL 0.006 M CH_3COONH_4 (pH = 6)	Na, Mg, Ca, P, S
e. Eluting with ~20 mL 3 M HNO_3	e. Eluting with 5 mL 1 M HNO_3	Ni, Cu, other trace metals

(pH = 6.0 ± 0.2) and eluted with 5 mL 1 M nitric acid (Table 1).

Nobias-PA1 resin was used to extract Ni and Cu as well as remove primary matrix in seawater (Table 1). Seawater samples (4 L) were acidified to pH = 1.8 with 4 mL concentrated distilled HCl, and left to equilibrate for several months. Ni and Cu were extracted from seawater using the two-step protocol described by Conway et al., 2013. 2.5 mL pre-cleaned Nobias PA1 resin was added to pH = 1.8 seawater and shaken overnight on a shaker table. The pH of the solution was increased to 6.0 ± 0.2 by addition an ammonium acetate buffer and shaken for ~5 h. Afterward, the resin was filtered from the solution by pouring through an acid-washed, 8 μm polycarbonate filter (Whatman), rinsed thoroughly with Milli-Q water and eluted in ~20 mL 3 M nitric acid (Conway et al., 2013).

Preconcentrated seawater samples were evaporated to dryness on a hot plate overnight, digested with 200 μL 1:1 HCl:HNO_3 for > 2 h, and evaporated to dryness again. To separate samples in series with published Fe, Zn, and Cd protocols (Conway et al., 2013), the seawater sample was redissolved in 10 M HCl with 0.011% H_2O_2 and loaded onto microcolumns containing AG-MP1 resin (100–200 mesh). Cu and Ni were eluted into the same vial with successive elutions of 10 M HCl (150 μL total) and 5 M HCl (300 μl total) and dried down at 105 °C. We note that this first chromatography step is only necessary for obtaining purified Fe, Zn and Cd fractions; investigators interested only in the purification of Ni and Cu should skip this step.

Samples were then processed with the protocol shown in Fig. 1 and Tables 1–4 to separate Ni and Cu and remove elements that have the potential to bias the isotopic analysis. Ni and Cu are first separated from each other by using 0.25 mL AG-MP1 (100–200 mesh) exchange resin. Ni is eluted with 15 M acetic acid + 1.2 M HCl and Cu is eluted with 5 M HCl (Fig. 3, Table 2). The Cu fraction is further purified by the same resin and column, rinsed with 22 M methanol + 0.9 M hydrobromic acid and eluted in 1 M HF (Fig. 4, Table 3). The Ni fraction is purified with 0.6 mL Nobias-PA1 resin, rinsed with ammonium acetate, eluted in 1 M nitric acid, and then by the same procedure for Ni and Cu separation (Figs. 2 and 3, Table 4). All procedures with AG-MP1 and Nobias-PA1 resin were performed with Bio-Spin® Disposable Chromatography Columns. After purification, the Ni and Cu elution fractions were collected and evaporated to dryness in 7 mL PFA vials, then refluxed in 1 mL of 14 M HNO_3 and 0.1 mL of 35% H_2O_2 at 160 °C for at least 6 h to decompose any leftover organic matter (Yang et al., 2019). The samples were evaporated to dryness again and were re-dissolved with 0.1 M HNO_3 to achieve a final concentration of approximately 300 ppb Ni or 50 ppb Cu for isotopic analysis. To measure the elemental composition of purified Ni and Cu samples, a small portion of sample aliquot was taken and diluted in 0.5 M HNO_3. The protocol of sample handling and analysis is shown by a flowchart in Fig. 1.

Table 2
Protocol for separating Ni and Cu in trace metal extracts by AG-MP1 resin.

Step	Reagent	Volume	Collection
Loading AG-MP1 resin into columns		0.25 mL	
Cleaning resin	2 M HNO_3	2 mL	
Rinsing	Milli-Q	0.5 mL	
Conditioning	15 M CH_3COOH + 1.2 M HCl + 0.003% H_2O_2	0.4 mL × 2	
Sample loading	Sample (15 M CH_3COOH + 1.2 M HCl + 0.003% H_2O_2)	0.5 mL	Ni
Ni elution	15 M CH_3COOH + 1.2 M HCl + 0.003% H_2O_2	0.25 mL × 4	Ni, Cr
Matrix removal	15 M CH_3COOH + 1.2 M HCl + 0.003% H_2O_2	0.5 mL × 8	Ti, Cr
Cu elution	5 M HCl + 0.003% H_2O_2	0.4 mL × 16	Cu, Ti, Mn
Fe elution[a]	1 M HCl	0.2 mL × 14	Fe, Mo
Zn elution[a]	2 M HNO_3 + 0.1 M HBr	0.2 mL × 12	Zn, Sn
Cd elution[a]	2 M HNO_3	0.2 mL × 10	Cd

[a] Steps following Yang et al. (2019).

Table 3
Protocol for final purification of Cu by AG-MP1 resin.

Step	Reagent	Volume	Collection
Loading AG-MP1 resin into columns		0.25 mL	
Cleaning resin	2 M HNO_3	2 mL	
Rinsing	Milli-Q	0.5 mL	
Conditioning	22 M methanol + 0.9 M HBr	0.4 mL × 2	
Sample loading	Sample (22 M methanol + 0.9 M HBr)	1 mL	Ti, Mn, Cr
Matrix removal	22 M methanol + 0.9 M HBr	1 mL × 5	Ti, Mn, Cr
Cu elution	1 M HF + 0.003% H_2O_2	1 mL × 5	Cu
Leftover	2 M HNO_3	1 mL × 5	Ti

2.3. Instrumentation and mass spectrometry

Elemental analysis was carried out by a Thermo Element 2 ICPMS using a 100 μL min^{-1} Teflon nebulizer, glass cyclonic spray chamber with a PC^3 Peltier cooled inlet system (ESI), standard Ni sampler and Ni 'H-type' skimmer cones at the department of Earth Sciences of University of Southern California. The sensitivity and stability of the instrument was tuned to optimal conditions before analysis. The analysis was conducted with sensitivity around 10^6 counts s^{-1} for 1 ppb In.

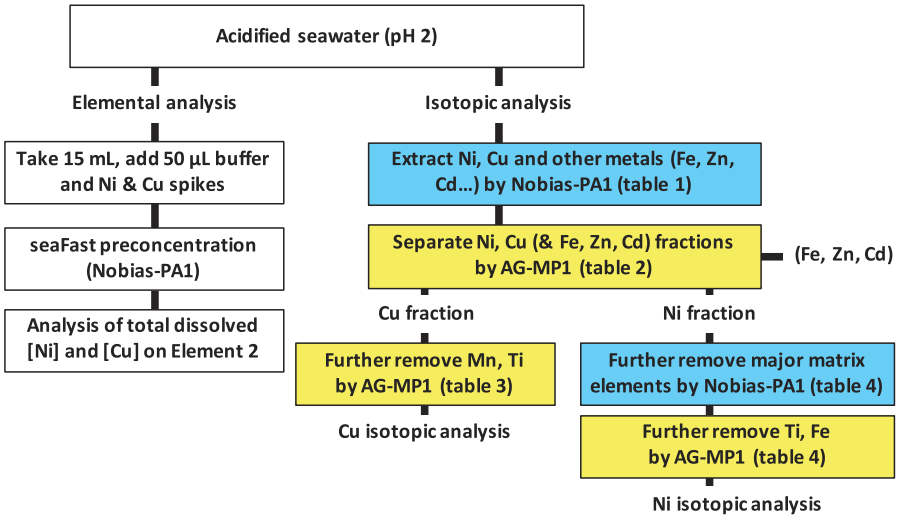

Fig. 1. Flowchart of sample handling and analysis. Highlighted steps are outlined in Tables 1–4.

Table 4
Protocols for final purification of Ni.

Step	Reagent	Volume	Collection
Loading Nobias-PA1 resin into columns		0.6 mL	
Cleaning resin	1 M HNO_3	5 mL	
Rinsing	Milli-Q	0.5 mL	
Conditioning	0.05 M CH_3COONH_4 (pH = 6)	0.5 mL × 2	
Sample loading	Sample (0.05 M CH_3COONH_4, pH = 6)	0.5 mL	Na, Mg, Ca, P, S
Matrix removal	0.006 M CH_3COONH_4 (pH = 6)	1 mL × 5	Na, Mg, Ca, P, S
Ni elution	1 M HNO_3	1 mL × 5	Ni
Loading AG-MP1 resin into columns		0.25 mL	
Cleaning resin	2 M HNO_3	2 mL	
Rinsing	Milli-Q	0.5 mL	
Conditioning	15 M CH_3COOH + 1.2 M HCl + 0.003% H_2O_2	0.4 mL × 2	
Sample loading	Sample (15 M CH_3COOH + 1.2 M HCl + 0.003% H_2O_2)	0.5 mL	Ni
Ni elution	15 M CH_3COOH + 1.2 M HCl + 0.003% H_2O_2	0.25 mL × 4	Ni

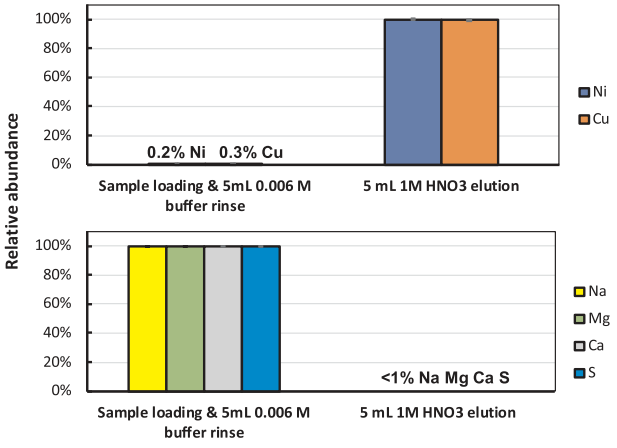

Fig. 2. Recovery of Ni, Cu and major elements during preconcentration with Nobias-PA1 resin. A multi-element standard containing 100 ng Ni, Cu, Na, Mg, Ca, P and S was dried and re-dissolved in in 0.5 mL 0.05 M ammonium acetate (pH = 6) and loaded onto Nobias-PA1 resin. Bars show relative abundance of elements eluted during a combined loading and rinsing step, and during acid elution. Recoveries reflect duplicate tests.

Both the standard and samples were doped with 1 ppb In to correct for shifts in instrumental sensitivity and matrix. Elemental concentrations in samples were determined by their signal intensity compared to a 10 ppb multi-element standard, which was diluted from a certified standard (Santa Clarita).

The isotopic composition of Ni and Cu (δ^{60}Ni and δ^{65}Cu) were measured on a Thermo Neptune Plus MC-ICPMS at the institute of Earth Sciences, Academia Sinica, Taiwan. Jet sampler and 'x-type' skimmer cones were used to maximize sensitivity. Standards and samples were introduced through a 100–150 μL min^{-1} Teflon nebulizer using a double-pass cyclonic spray chamber.

Instrumental settings and data acquisition method followed Takano et al. (2017). Briefly, Ni and Cu were measured in 'high resolution' mode, using a high resolution slit (25 μm), in order to resolve polyatomic isobaric interferences. For Ni measurements, ^{58}Ni, ^{60}Ni, ^{61}Ni and ^{62}Ni were simultaneously measured in each analysis, along with ^{57}Fe to correct the interference by ^{58}Fe, and ^{63}Cu and ^{65}Cu to account for instrumental mass bias. δ^{65}Cu was determined by monitoring ^{63}Cu and ^{65}Cu, as well as ^{69}Ga and ^{71}Ga to account for instrumental mass bias. Data collection consisted of 30 4.2 s cycles. Pure 0.1 M HNO_3 solution was measured every 4–6 samples to determine background signals,

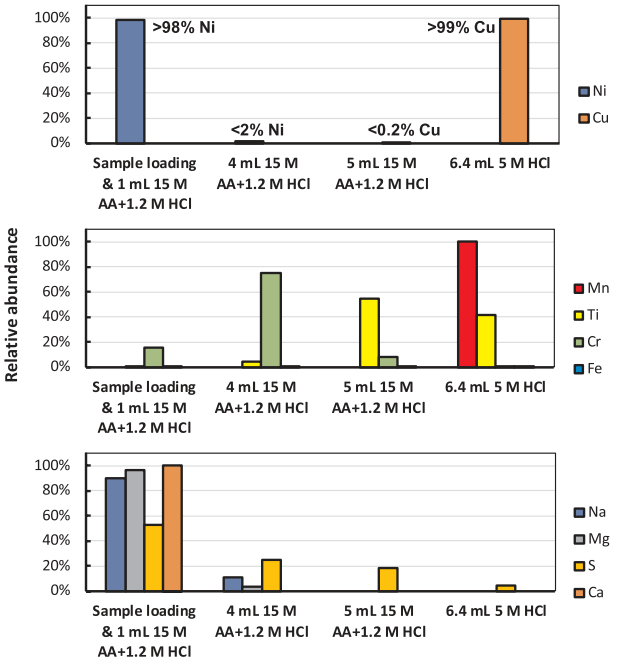

Fig. 3. Separation of Ni and Cu fractions. Recoveries of Ni, Cu, interfering elements Mn, Ti, Cr, Fe, and matrix elements Na, Mg, Ca and S from the purification protocol in Table 2. For this comparison, a multi-element standard with 100 ng of each element was resuspended in 15 M acetic acid (AA) + 1.2 M HCl eluent and loaded on AG-MP1 resin. All reagents also contain 0.003% H_2O_2.

which were then subtracted from sample intensities. Standards were also measured routinely, every 4–6 samples, to correct potential systematic drift during each session. Isotope ratios are expressed in per mil (‰) relative to the average of the primary standards NIST 986 Ni and NIST 976 Cu, respectively, using delta notation calculated as follows;

$$\delta^{60}\mathrm{Ni} = \left[\frac{(^{60}\mathrm{Ni}/^{58}\mathrm{Ni})_{\mathrm{sample}}}{(^{60}\mathrm{Ni}/^{58}\mathrm{Ni})_{\mathrm{NIST\ SRM\ 986}}} - 1\right] \times 10^3$$

$$\delta^{65}\mathrm{Cu} = \left[\frac{(^{65}\mathrm{Cu}/^{63}\mathrm{Cu})_{\mathrm{sample}}}{(^{65}\mathrm{Cu}/^{63}\mathrm{Cu})_{\mathrm{NIST\ SRM\ 976}}} - 1\right] \times 10^3$$

The accuracy of our analytical conditions was verified by determining the isotope composition of multiple secondary standards for each element on the same day. Ni standard Wako Ni was −0.27 ± 0.08‰ (2σ, n = 10), which is consistent with the value reported by Takano et al. (2017) (−0.28 ± 0.03‰.). NIST SRM 3114 Cu was −0.07 ± 0.11‰ (2σ, n = 6) and Cu standard Wako Cu was +0.27 ± 0.05‰ (2σ, n = 5). These values are statistically consistent with values reported previously (−0.06 ± 0.02‰ by Baconnais et al., 2019 and +0.28 ± 0.03‰ by Takano et al., 2017, respectively).

Long-term reproducibility of Ni and Cu isotopic analyses is ± 0.08‰ (n = 21; over ~1 year) and ± 0.07‰ (n = 65; over 2 years), respectively, which was assessed over the course of this and parallel studies through repeated measurements of primary NIST standards and secondary standards Wako Ni and Wako Cu. The internal precision of single measurement ranged from ± 0.05 to ± 0.08‰ for Ni and from ± 0.05 to ± 0.19‰ for Cu, which was obtained by combining the internal precision of both sample and standard measurements (Conway et al., 2013). The analytical reproducibility for the reported isotopic composition of each sample is the long-term reproducibility, unless the internal uncertainty is larger, in which case the latter is reported (Table S1).

2.4. Mass bias correction

We used Cu and Ga to correct the artificial isotopic fractionation of sample Ni and Cu isotope ratios caused by the mass spectrometer. NIST SRM 976 Cu standard was added in Ni samples to achieve a ratio of 300 ppb Ni: 300 ppb Cu, and an in-house Ga solution (VWR Chemicals BDH®) was used for Cu at a ratio of 50 ppb Cu: 100 ppb Ga. We note that because the method cannot correct potential isotopic fractionation by chromatographic separation on Ni and Cu samples, quantitative recovery during sample processing is essential (see Section 3.3).

3. Results and discussion

Below, we describe our new Ni and Cu purification protocols and their performance, including the separation of matrix elements and interfering elements, as well as the recovery of Ni and Cu and procedure blanks. This procedure is compatible with methods for separating Fe, Zn and Cd within a single seawater sample described in Conway et al., 2013 (Fig. S1). Finally, we present the isotope analyses for various reference materials and seawater samples purified with this new method.

3.1. Nobias-PA1 preconcentration

Before examining Cu and Ni recovery from seawater samples, we first tested Nobias-PA1 extraction of a multi-element standard with 100 ng of each element dissolved in 0.05 M ammonium acetate, which recovered 99.8 ± 0.3% Ni and 99.7 ± 0.1% Cu and removed over 99% of Na, Mg, Ca, and S, which made up the primary matrix in most natural samples (Fig. 2). The Cu and Ni recovery for large volume seawater samples by Nobias-PA1 was determined in two steps. First, 15 mL aliquots were taken from 4 L seawater samples, spiked with a solution containing ^{62}Ni and ^{65}Cu, automatically preconcentrated using a seaFAST Pico system (Elemental Scientific) with Nobias PA-1 resin, and analyzed by an Element 2 ICP-MS to determine total dissolved Ni and Cu concentrations. Using this method, Cu and Ni concentrations for GEOTRACES reference seawater GSP was determined to be 2.53 nM Ni and 0.60 nM Cu GSP, which agrees with average values from a recent intercomparison (2.60 ± 0.10 nM Ni and 0.574 ± 0.053 nM Cu) (www.geotraces.org/standards-and-reference-materials/).

Ni and Cu in 4 L samples were then preconcentrated by the batch extraction protocol described in Section 2.2. A small portion of the extracts were taken and spiked with ^{62}Ni and ^{65}Cu spikes and measured by Element 2 ICP-MS. The comparison between extractable (large volume samples) and total dissolved concentrations (extracted by SeaFAST) yielded recoveries of 102 ± 3% for Ni and 86 ± 3% for Cu (2σ). Incomplete extraction of Cu may result from strong ligands in seawater and can introduce bias into Cu isotopic measurements if Cu bound to strong ligands is isotopically distinct from extractable Cu. Although UV oxidation of large volume samples is extraordinarily cumbersome, this procedure is ultimately needed to evaluate whether or not isotopic disequilibrium exists between Cu bound to strong ligands and the remainder of the Cu pool. Recently, multiple studies have highlighted a need to revisit seawater extraction protocols to improve Cu recovery (Posacka et al., 2017; Little et al., 2018) and a seawater Cu isotope intercalibration effort is ongoing. Regardless, because our measurements overlap with published measurements of seawater δ^{65}Cu, we expect that incomplete sample recovery has not affected out results (see Section 3.7). We note that Cu recovery from all subsequent purification is quantitative (see Section 3.3).

Besides Ni and Cu, the extracts also contained 28–865 μg Na, 9–191 μg Mg, 23–1073 μg S, 1–109 μg Ca, 11–224 ng Fe, 22–176 ng Mn, 2–136 ng Ti and 2–13 ng Cr. Each of these elements can cause isobaric interferences on Ni and Cu isotopic analysis and their ranges may reflect variable concentrations in the original sample, or different degrees of rinsing during extraction. As a result, we designed the following procedure to further remove these elements from Ni and Cu samples.

3.2. Ni and Cu separation

From seawater extracts, Ni and Cu must be purified of interfering elements and, ideally, separated from each other. Our previous study has shown that anion exchange chromatography using AG-MP1 resin with either 15 M acetic acid + 1.2 M HCl or 11 M acetic acid + 4 M HCl is able to separate Ti, Cr and Fe from Ni and Cu (Yang et al., 2019). Both protocols can yield > 98% recovery for Ni and > 99% recovery for Cu with < 1% Na, Mg and Ca in Cu fraction (Fig. 3). We adopted the 15 M acetic acid + 1.2 M hydrochloric acid protocol to process samples (Table 2) because it was more effective at removing Ti from the Ni fraction (Fig. 3). Although this protocol results in higher Ti, 100% Mn and ~ 4% S recoveries in the Cu fraction, these elements can be quantitatively separated by a second column chemistry described below (Table 3). This protocol can be performed in approximately 1 h.

3.3. Cu purification

We developed a novel protocol by using AG-MP1 resin to further isolate Cu from undesirable elements based on two key observations. First, in a solution of 22 M methanol + 0.9 M HBr, the resin will retain Cu but not Mn and S. Second, AG-MP1 will retain Ti in a 1 M HF solution, but Cu will be eluted. This approach was inspired by studies published over half century ago that explored trace metal adsorption onto strongly basic anion-exchange resins in various organic and non-organic solvents including methanol and hydrochloric, hydrofluoric and hydrobromic acids. Studies with Dowex 1 × 8 resin showed that the resin could tightly bind Cu in methanol-HBr mixture (distribution coefficient > 1000) with almost no adsorption of Mn, Ti and Cr (Korkisch and Hazan, 1965; Klakl and Korkisch, 1969). A similar resin, Dowex 1 × 10, was also studied and found to retain Ti, but not Cu, in 1 M HF (Faris, 1960; Nelson et al., 1960).

The Cu purification procedure is described below. Aliquots of the Cu fraction (the product of Section 3.2) were evaporated to dryness and redissolved in 1 mL 22 M methanol + 1.2 M HCl. After cleaning and conditioning the AG-MP1 resin with 5 mL 2 M HNO_3, 0.5 mL Milli-Q water and 0.8 mL 22 M methanol + 1.2 M HCl, the sample was loaded onto the column and resin was then rinsed with 5 mL 22 M methanol + 1.2 M HCl to fully remove Mn and S. Cu was then eluted with 5 mL 1 M HF (Table 3). The protocol takes 1 h to finish and can yield 99.7 ± 0.2% Cu recovery with ≤1% Mn and Ti and ~6% S based on testing on a multi-element standard (Fig. 4). Ignoring the incomplete recovery of Cu from seawater during Nobias-PA1 preconcentration, the combined Cu recovery of the protocols for seawater samples was 105 ± 7%. The larger uncertainty here derives from reduced precision associated with external calibration of Cu concentration by MC-ICPMS compared to isotope dilution via Element 2.

3.4. Ni purification

As described in Section 3.1, Nobias-PA1 preconcentration of seawater can still allow μg levels of major matrix elements existing in trace metal extracts. In the Ni and Cu separation protocol (Section 3.2), these elements are partitioned into Ni fraction (Fig. 3). To avoid their interference on Ni isotopic analysis, a second Nobias-PA1 purification was carried out to isolate Ni from the elements (Table 4), which takes around 1 h. Because extended processing can lead to inadvertent contamination of Fe and other metals that are also extracted by Nobias-PA1, a final Ni separation procedure was performed. This follows the same AG-MP1 separation protocol from Section 3.2 (Table 4) and takes ≤1 h to perform. External calibration (beam intensity matching) during δ^{60}Ni analysis indicated that overall Ni recovery from these protocols was 96 ± 11%.

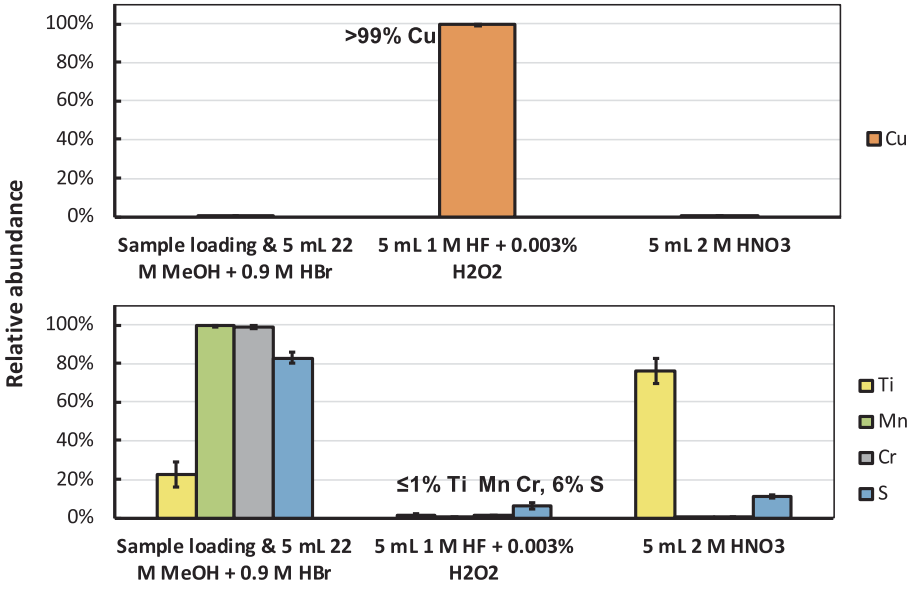

Fig. 4. Final copper purification. Recoveries of Cu, Ti, Mn, Cr, and S from the Cu purification protocol in Table 3. For this comparison, a multi-element standard containing 100 ng of each element was dissolved in 0.5 to 1 mL of 22 M methanol (MeOH) + 0.9 M hydrobromic acid (HBr) and loaded onto AG-MP1 resin. Bars represent average recovery from triplicate tests.

3.5. Blanks

Overall procedural blanks (including Nobias-PA1 extraction, Ni and Cu separation and purification) were ≤ 1 ng Ni and Cu, which is equivalent to ≤4 pM Ni and Cu in a 4 L seawater samples. Compared to the concentrations of samples we processed, 2.1–6.3 nM Ni (120–375 ng) and 0.5–1.7 nM Cu (30–110 ng), these blanks are negligible.

3.6. Validation of purification method

We used reference materials including BCR-414 (plankton), Arizona Test Dust (continental sediments), PACS-2 and MESS-3 (marine sediments) to test our purification method (Table 5). The high Fe, Mn, Ti and Cr content of these samples allows the merit of this method to be demonstrated. For example, the marine plankton sample BCR-414 contains around 2000 ppm Fe, 300 ppm Mn, 100 ppm Ti and 25 ppm Cr while the Ni and Cu contents are approximately 20 and 30 ppm, respectively. Following purification, these elements were all < 1 ppb while recovery of Ni and Cu were over 99%. Isotopic analysis yielded values of δ^{60}Ni = +0.07 ± 0.06‰ and δ^{65}Cu = −0.29 ± 0.10‰ in BCR-414 (2σ, *n* = 3). These are consistent with the values of δ^{60}Ni = +0.11 ± 0.06‰ and δ^{65}Cu = −0.27 ± 0.05‰ published by Takano et al. (2020).

Table 5
δ^{60}Ni and δ^{65}Cu in pure standards and reference materials.

Material		Result in this study		Reference value
Ni	*Type*	*δ^{60}Ni ± 2σ (‰)*	*n*	*δ^{60}Ni ± 2σ (‰)*
Wako	Pure standard	−0.29 ± 0.08	21	−0.28 ± 0.03[a]
BCR-414	Plankton	+0.07 ± 0.06	3	+0.11 ± 0.06[b]
PACS-2	Marine sediment	+0.19 ± 0.10	1	
MESS-3	Marine sediment	−0.04 ± 0.09	1	
Arizona test dust	Natural soil	−0.09 ± 0.10	1	
Cu	*type*	*δ^{65}Cu ± 2σ (‰)*	*n*	*δ^{65}Cu ± 2σ (‰)*
NIST SRM 3114	Pure standard	−0.07 ± 0.04	6	−0.06 ± 0.02[c]
Wako	Pure standard	+0.27 ± 0.07	65	+0.28 ± 0.03 [a]
BCR-414	Plankton	−0.29 ± 0.10	3	−0.27 ± 0.05[b]
PACS-2	Marine sediment	0.00 ± 0.07	3	+0.05 ± 0.06[d]
MESS-3	Marine sediment	−0.12 ± 0.10	3	0.00 ± 0.10[d]
Arizona test dust	Natural soil	+0.14 ± 0.08	3	

[a] Takano et al. (2017).
[b] Takano et al. (2020).
[c] Baconnais et al. (2019).
[d] Araújo et al. (2019).

Cu isotope values for marine sediment standards PACS-2 and MESS-3 were determined to be 0.00 ± 0.07‰ and −0.12 ± 0.10‰, respectively (2σ, n = 3). These results agree with values published by Araújo et al. (2019) of +0.05 ± 0.06‰ for PACS-2 and 0.00 ± 0.10‰ for MESS-3. Furthermore, we report δ^{65}Cu of Arizona Test Dust to be +0.14 ± 0.08‰ (2σ, n = 3). We are unaware of published measurements of this material, although our determination overlaps with δ^{65}Cu values for igneous rocks and clastic sediments (+0.08 ± 0.17‰ and +0.08 ± 0.20‰, respectively; compiled by Moynier et al., 2017). δ^{60}Ni values for PACS-2, MESS-3 and Arizona Test Dust were determined to be +0.19 ± 0.10‰, −0.04 ± 0.09‰, and −0.09 ± 0.10‰ (2σ, *n* = 1), respectively, and are reported for the first time in this study. We note that these values overlap with the isotopic ranges of continental sediments (soil, loess and river sediment; −0.04 ± 0.02‰ to +0.23 ± 0.08‰) and deep-sea sediments (clay; +0.02 ± 0.03‰ and +0.04 ± 0.04‰) (Cameron et al., 2009; Cameron and Vance, 2014; Ratié et al., 2015). As PACS-2, MESS-3 and Arizona Test Dust have different origins (harbor sediments, offshore sediments and nature soils, respectively), the slight differences in δ^{60}Ni among the materials might reflect different geologic processes.

3.7. Dissolved nickel and copper isotopic composition in the North Pacific

Seawater samples from the upper water column of the North Pacific Ocean were collected on the Gradients cruise in April 2016 and were analyzed for Ni and Cu concentration and isotopic composition (Figs. 5 and 6; Table S1). Both elements have a similar distribution, with elevated concentrations at the northern end of the transect (36°N) due to an upwelling source from deep waters. Lower concentrations were observed in subtropical surface waters further south. The general features of the Ni and Cu distributions along this transect were similar to nitrate, phosphate, and other phytoplankton macronutrients. In surface waters, however, latitudinal gradients of Ni and Cu were less intense than observed for macronutrients, indicating slower rates of uptake and/or export relative to physical mixing (Foreman et al., 2020).

Dissolved Ni (dNi) in the deepest samples (600 m) had a uniform isotopic composition of +1.37 ± 0.08‰ (2σ; n = 3). Toward the

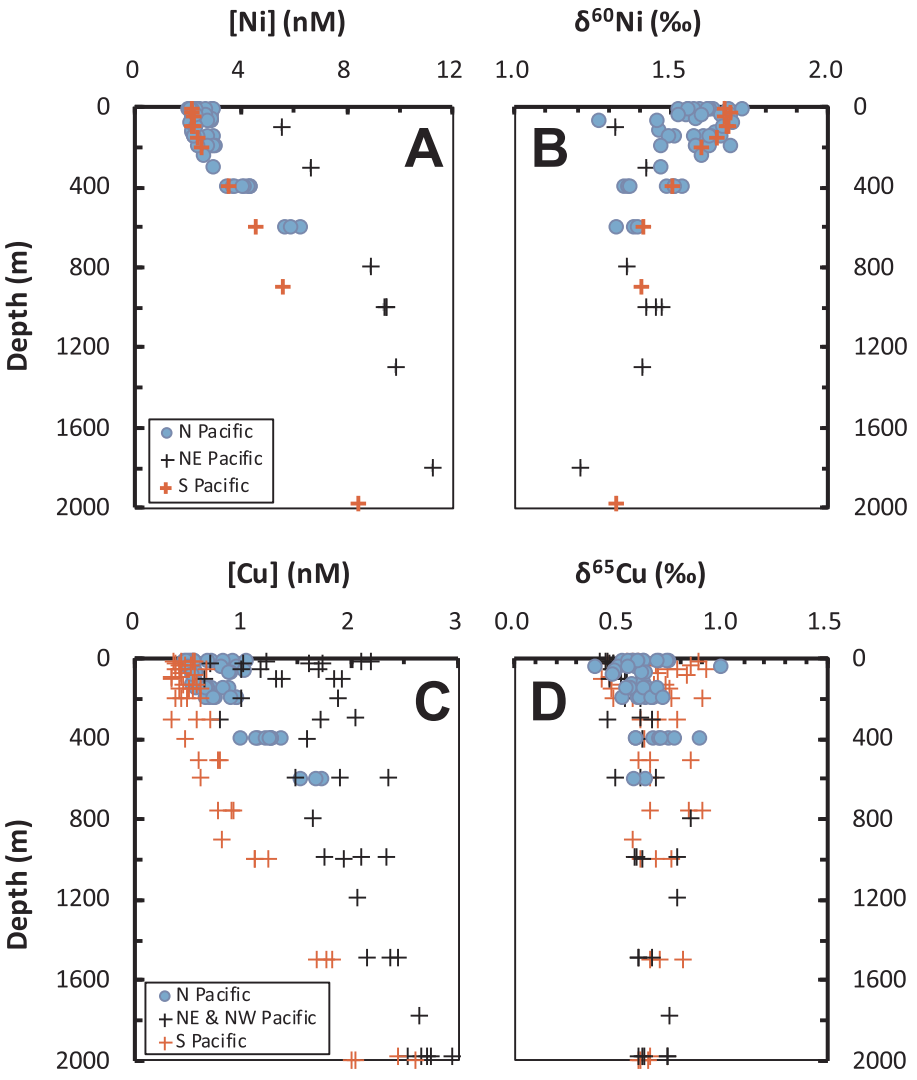

Fig. 5. Profiles of dissolved Ni concentration (A), dissolved δ^{60}Ni (B), dissolved Cu concentration (C) and dissolved δ^{65}Cu (D) from the Pacific Ocean. Blue circle shows seawater samples collected on the Gradients expedition (April 2016). Black crosses in A and B represent data from the NE Pacific (Cameron and Vance, 2014) and red cross represent data from the S Pacific (Takano et al., 2017). In C and D, black cross represent NE and NW Pacific data from Takano et al. (2014) and red crosses represent S Pacific data from Thompson and Ellwood (2014) and Takano et al. (2017). (For interpretation of the references to colour in this figure legend, the reader is referred to the web version of this article.)

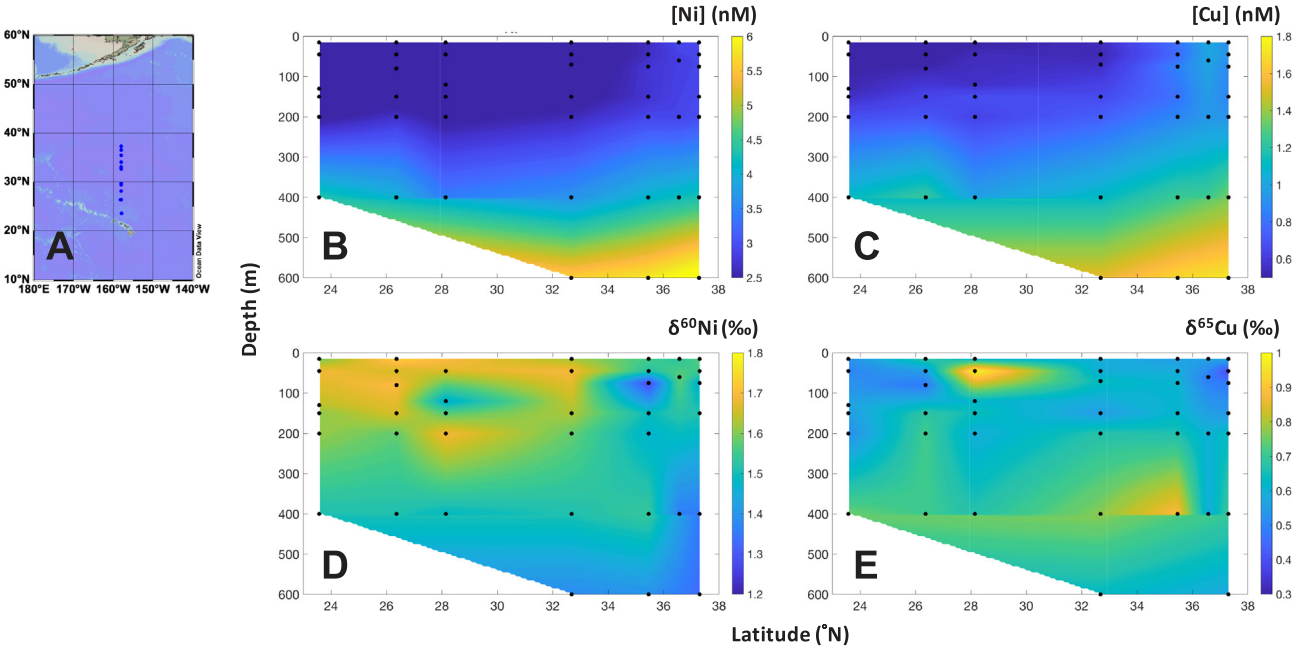

Fig. 6. Sampling locations (A), dissolved Ni concentration (B), dissolved Cu concentration (C), dissolved δ^{60}Ni (D) and dissolved δ^{65}Cu (E) from the Gradients transect in the North Pacific Ocean.

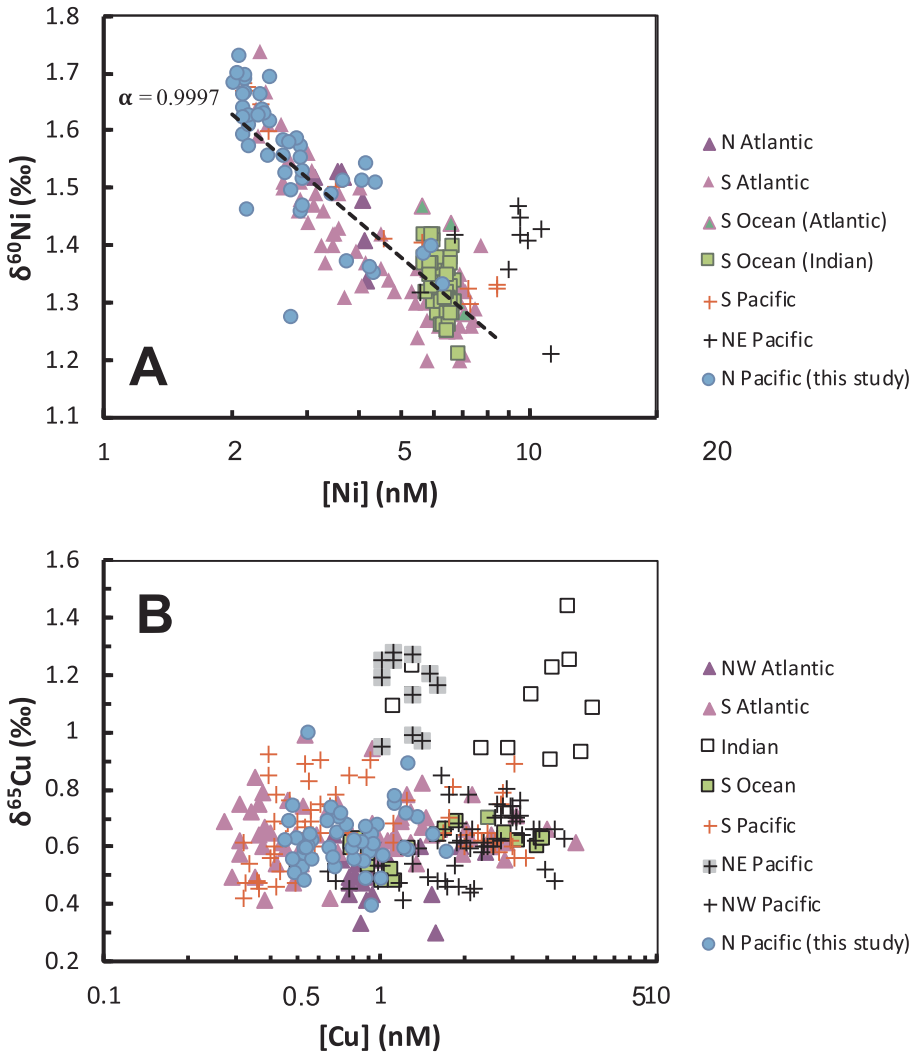

Fig. 7. Compilation of dissolved δ^{60}Ni (A) and dissolved δ^{65}Cu measurements (B) from the global ocean.
Data sources for Ni include Cameron and Vance (2014) (N Atlantic and NE Pacific), Takano et al. (2017) (S Pacific), Wang et al. (2019) (Southern Ocean) and Archer et al. (2020) (S Atlantic and Southern Ocean). Literature Cu data originates from Vance et al. (2008) (NE Pacific and Indian Ocean), Thompson and Ellwood (2014) (S Pacific), Takano et al. (2014) (Southern Ocean and NW Pacific), Takano et al. (2017) (S Pacific), Little et al. (2018) (S Atlantic), Boyle et al. (2012) (NW Atlantic) and Baconnais et al. (2019) (NE Atlantic).

surface, δ^{60}Ni increased in all subtropical stations, reaching a maximum of +1.73 ± 0.08‰ in surface waters, where dNi was at a minimum. With the exception of a few outliers, this pattern of higher δ^{60}Ni for decreasing dNi applied to the entire dataset. Indeed, we observed a correlation between δ^{60}Ni and the natural log of dNi (R^2 = 0.59; Fig. 7a), which can be explained by a closed system fractionation model whereby phytoplankton preferentially acquire light Ni isotopes after subsurface waters are brought into the euphotic zone, analogous to a Rayleigh distillation process (Ripperger et al., 2007). Least squares regressions indicate that a fractionation factor $\alpha_{bio\text{-}sw}$ of 0.9997 ± 1 (2σ) best explains the change in δ^{60}Ni along the section. This value is similar to the range of fractionation factors observed by phytoplankton in culture for uptake of Cd^{2+} (0.9986–0.9996: Lacan et al., 2006; John and Conway, 2014; Horner et al., 2013) and Zn^{2+} (0.9992–0.9998: John et al., 2007; John and Conway, 2014; Samanta et al., 2018), and suggest that the binding of divalent metals to transporters may drive similar fractionation in all three cases. We note that Ni uptake by methanogens also results in Ni isotope fractionation of a similar magnitude and direction (α ≈ 0.9992; Cameron et al., 2009).

The biological removal of light Ni isotopes observed on the Gradients dataset is consistent with δ^{60}Ni profiles in the South Pacific (Takano et al., 2017) and South Atlantic Oceans (Archer et al., 2020), which show a 0.4‰ increase in δ^{60}Ni associated with a 5–6 nM decrease in dNi. Both locations are marked with a surface δ^{60}Ni of +1.7‰, similar to our measurements (Fig. 5a and b). It is interesting that such fractionation is not observed in the Subarctic North Pacific (Cameron and Vance, 2014), further north of the Gradients transect, or in the Southern Ocean (Wang et al., 2019; Archer et al., 2020). In these cases, δ^{60}Ni is uniform in the water column at approximately +1.4‰, even though dNi uptake in the surface ocean was observed. While an ongoing Ni isotope intercalibration will add confidence to these isotopic differences, it is possible that Ni isotope fractionation may be localized in subtropical environments. Widespread Ni enzymes such as the Ni superoxide dismutase (Ni-SOD) and urease are likely more important in lower latitudes where both solar irradiation and nitrogen recycling are intense (Price and Morel, 1991; Dupont et al., 2008). These environments also harbor diazotrophic cyanobacteria such as *Trichodesmium*, which require more Ni than other phytoplankton groups due to increased demand for Ni-SOD, as well as uptake hydrogenase (Ho, 2013; Rodriguez and Ho, 2014). High demand and slow coordination kinetics may motivate the production of high affinity Ni transporters (Hudson and Morel, 1993; Dupont et al., 2012), possibly leading to isotopic

fractionation. Alternatively, phytoplankton Ni fractionation may occur globally, but is overwritten in high latitude oceans due to different isotope effects associated with Ni incorporation into diatom frustules (Twining et al., 2012) or an altered Ni binding environment due to the presence of competing metals (Egleston and Morel, 2008).

Unlike Ni, the δ^{65}Cu of dissolved Cu (dCu) is relatively uniform and does not show strong evidence for fractionation during biological uptake. Despite a two-fold difference in deep and shallow dCu concentrations, the δ^{65}Cu of 10 samples with the lowest dCu concentration (+0.59 ± 0.16‰ and 0.59 ± 0.06 nM, 2σ) was statistically indistinguishable from the δ^{65}Cu from 10 samples with the highest dCu (+0.69 ± 0.21‰ and 1.35 ± 0.44 nM, 2σ). Our measurements of δ^{65}Cu also overlap with published measurements, which mostly fall between +0.4 and +0.8‰ (Fig. 7b; Thompson and Ellwood, 2014; Takano et al., 2014, 2017; Little et al., 2018; Boyle et al., 2012; Baconnais et al., 2019), despite incomplete extraction of Cu from seawater with Nobias PA-1 resin (average recovery from this sample set is 86%). Recently, Little et al. (2018) reported no significant difference in δ^{65}Cu between samples with 'good' and 'poor' recovery. However, extraction of Cu by magnesium hydroxide co-precipitation appears to result in systemically heavier δ^{65}Cu (Vance et al., 2008) compared to samples extracted with Nobias PA-1 resin (Fig. 7b).

Limited variability of δ^{65}Cu in our dataset and from other ocean basins indicates that net isotopic fractionation associated with biological uptake, remineralization, and scavenging is probably insignificant. This may reflect the important role of organic ligands in the marine Cu cycle, which probably have masses of several hundred Daltons (Dupont et al., 2004; Boiteau et al., 2016), and the fact that phytoplankton may take up ligand-bound Cu directly (Semeniuk et al., 2015). Complexation with ligands makes the relative mass difference between ^{63}Cu and ^{65}Cu extremely small, potentially making mass dependent fractionation insignificant for Cu-ligand complexes. In contrast, electrochemical studies indicate that only a fraction of dNi is bound by ligands (< 50%), allowing a high concentration of inorganic Ni species (Achterberg and Van Den Berg, 1997; Saito et al., 2004; Boiteau et al., 2016). Therefore, isotopic fractionation associated with Ni uptake may indicate direct uptake of Ni^{2+}, while the lack of fractionation associated with Cu uptake may indicate uptake by organic Cu complexes. Similarly, muted biological fractionation of Fe and Zn isotopes in the open ocean may reflect their association with organic ligands (Bruland, 1989; Rue and Bruland, 1995; Conway and John, 2014, Conway and John, 2015).

Despite the lack of systematic change in δ^{65}Cu, there is some evidence in our dataset for coherent variation in Cu isotopic composition near the surface ocean. Negative excursions in δ^{65}Cu in top 100 m to +0.4‰ are observed at the two northern-most stations of the Gradients transect (36.6 and 37.3°N). Slight decreases in δ^{65}Cu are also found at the southern end of our transect (23°N). Hints of similar effects are also observed in published Cu isotope profiles (Takano et al., 2014, 2017; Little et al., 2018). We anticipate that high resolution studies associated with GEOTRACES sections will provide more conclusive documentation of these features and identify their origin.

4. Conclusion

We have developed a new method for purification of Ni and Cu from seawater samples that is suitable for measurement of their stable isotope ratios. The method successfully recovers Ni and Cu after preconcentration from the seawater matrix, and separates these metals from other major and minor matrix elements that can interfere with analysis. The most notable improvement in this method compared to previous techniques is the ability to effectively purify Ni and Cu from Ti, Mn and Cr, ensuring accurate measurements of δ^{60}Ni and δ^{65}Cu. This method can be applied to diverse environmental and geological sample types that contain high levels of Ti, Mn and Cr.

Application of this method to 49 samples in the North Pacific has revealed consistent fractionation of δ^{60}Ni due to biological Ni uptake, supporting observations by Takano et al. (2017) and Archer et al. (2020). Tandem Ni and Cu isotope measurements also highlight the lack of Cu isotope fractionation in these waters, despite similar magnitudes of Ni and Cu uptake by phytoplankton.

This new method has the potential to greatly increase the throughput of Ni and Cu isotope measurement and is suitable for sectional studies, such as GEOTRACES transects. Each column protocol takes ~1 h to process and all of the resins are reusable. The relative speed and simplicity of this procedure are also conducive to automation with commercially available chromatography systems. Because this technique can be coupled with purification of Fe, Zn, and Cd (Conway et al., 2013), isotopic measurement of at least five metals can be performed from on a single seawater sample (Table 2, Fig. S1).

Declaration of competing interest

The authors declare that they have no known competing financial interests or personal relationships that could have appeared to influence the work reported in this paper.

Acknowledgement

We would like to thank Shotaro Takano for providing pure Ni and Cu isotope standards, and Irit Tal and Wen-Hsuan Liao for technical support. We acknowledge the Captain and Crew of the R/V Ka'imikai-O-Kanaloa, Chief Scientist E. Virginia Armbrust and Ryan Tabata for sampling support. This work was supported by the Simons Foundation (SCOPE award 329108 to S.G.J., Gradients award 426570SP to S.G.J., and 602538 to N.J.H.), the National Science Foundation (NSF-OCE 1736896 to S.G.J.), and the Taiwan-USC Postdoctoral Fellowship Program (S.C.Y.). We also thank the Editor and two anonymous referees for their helpful comments.

Appendix A. Supplementary data

Supplementary data to this article can be found online at https://doi.org/10.1016/j.chemgeo.2020.119662.

References

Achterberg, E.P., Van Den Berg, C.M., 1997. Chemical speciation of chromium and nickel in the western Mediterranean. Deep-Sea Res. II Top. Stud. Oceanogr. 44 (3–4), 693–720.

Araújo, D.F., Ponzevera, E., Briant, N., Knoery, J., Sireau, T., Mojtahid, M., Metzger, E., Brach-Papa, C., 2019. Assessment of the metal contamination evolution in the Loire estuary using Cu and Zn stable isotopes and geochemical data in sediments. Mar. Pollut. Bull. 143, 12–23.

Archer, C., Vance, D., 2004. Mass discrimination correction in multiple-collector plasma source mass spectrometry: an example using Cu and Zn isotopes. J. Anal. At. Spectrom. 19 (5), 656–665.

Archer, C., Vance, D., Milne, A., Lohan, M.C., 2020. The oceanic biogeochemistry of nickel and its isotopes: New data from the South Atlantic and the Southern Ocean biogeochemical divide. Earth Planet. Sci. Lett. 535, 116–118.

Baconnais, I., Rouxel, O., Dulaquais, G., Boye, M., 2019. Determination of the copper isotope composition of seawater revisited: a case study from the Mediterranean Sea. Chem. Geol. 511, 465–480.

Bermin, J., Vance, D., Archer, C., Statham, P.J., 2006. The determination of the isotopic composition of Cu and Zn in seawater. Chem. Geol. 226 (3–4), 280–297.

Boiteau, R.M., Till, C.P., Ruacho, A., Bundy, R.M., Hawco, N.J., McKenna, A.M., Barbeau, K.A., Bruland, K.W., Saito, M.A., Repeta, D.J., 2016. Structural characterization of natural nickel and copper binding ligands along the US GEOTRACES Eastern Pacific Zonal Transect. Front. Mar. Sci. 3, 243.

Borrok, D.M., Wanty, R.B., Ridley, W.I., Wolf, R., Lamothe, P.J., Adams, M., 2007. Separation of copper, iron, and zinc from complex aqueous solutions for isotopic measurement. Chem. Geol. 242, 400–414.

Boyle, E.A., Sclater, F.R., Edmond, J.M., 1977. The distribution of dissolved copper in the Pacific. Earth Planet. Sci. Lett. 37 (1), 38–54.

Boyle, E.A., Huested, S.S., Jones, S.P., 1981. On the distribution of copper, nickel, and cadmium in the surface waters of the North Atlantic and North Pacific Ocean. Journal of Geophysical Research: Oceans 86 (C9), 8048–8066.

Boyle, E.A., John, S., Abouchami, W., Adkins, J.F., Echegoyen-Sanz, Y., Ellwood, M., Flegal, A.R., Fornace, K., Gallon, C., Galer, S., Gault-Ringold, M., Lacan, F., Radic, A.,

Rehkamper, M., Rouxel, O., Sohrin, Y., Stirling, C., Thompson, C., Vance, D., Xue, Z., Zhao, Y., 2012. GEOTRACES IC1 (BATS) contamination-prone trace element isotopes Cd, Fe, Pb, Zn, Cu, and Mo intercalibration. Limnol. Oceanogr. Methods 10 (9), 653–665.
Bruland, K.W., 1980. Oceanographic distributions of cadmium, zinc, nickel, and copper in the North Pacific. Earth Planet. Sci. Lett. 47 (2), 176–198.
Bruland, K.W., 1989. Complexation of zinc by natural organic ligands in the central North Pacific. Limnol. Oceanogr. 34 (2), 269–285.
Cameron, V., Vance, D., 2014. Heavy nickel isotope compositions in rivers and the oceans. Geochim. Cosmochim. Acta 128, 195–211.
Cameron, V., Vance, D., Archer, C., House, C.H., 2009. A biomarker based on the stable isotopes of nickel. Proc. Natl. Acad. Sci. 106 (27), 10944–10948.
Ciscato, E.R., Bontognali, T.R., Vance, D., 2018. Nickel and its isotopes in organic-rich sediments: implications for oceanic budgets and a potential record of ancient seawater. Earth Planet. Sci. Lett. 494, 239–250.
Coale, K.H., Bruland, K.W., 1990. Spatial and temporal variability in copper complexation in the North Pacific. Deep Sea Research Part A. Oceanographic Research Papers 37 (2), 317–336.
Conway, T.M., John, S.G., 2014. Quantification of dissolved iron sources to the North Atlantic Ocean. Nature 511 (7508), 212–215.
Conway, T.M., John, S.G., 2015. The cycling of iron, zinc and cadmium in the North East Pacific Ocean–Insights from stable isotopes. Geochim. Cosmochim. Acta 164, 262–283.
Conway, T.M., Rosenberg, A.D., Adkins, J.F., John, S.G., 2013. A new method for precise determination of iron, zinc and cadmium stable isotope ratios in seawater by double-spike mass spectrometry. Anal. Chim. Acta 793, 44–52.
Dupont, C.L., Nelson, R.K., Bashir, S., Moffett, J.W., Ahner, B.A., 2004. Novel copper-binding and nitrogen-rich thiols produced and exuded by *Emiliania huxleyi*. Limnol. Oceanogr. 49 (5), 1754–1762.
Dupont, C.L., Barbeau, K., Palenik, B., 2008. Ni uptake and limitation in marine Synechococcus strains. Appl. Environ. Microbiol. 74 (1), 23–31.
Dupont, C.L., Johnson, D.A., Phillippy, K., Paulsen, I.T., Brahamsha, B., Palenik, B., 2012. Genetic identification of a high-affinity Ni transporter and the transcriptional response to Ni deprivation in Synechococcus sp. strain WH8102. Appl. Environ. Microbiol. 78 (22), 7822–7832.
Egleston, E.S., Morel, F.M., 2008. Nickel limitation and zinc toxicity in a urea-grown diatom. Limnol. Oceanogr. 53 (6), 2462–2471.
Faris, J.P., 1960. Adsorption of elements from hydrofluoric acid by anion exchange. Anal. Chem. 32 (4), 520–522.
Foreman, R.K., Ferron, S., Karl, D.M., 2020. Organic and inorganic nutrients in the North Pacific from the 2016 cruise KOK1606 (gradients 1) (version 1) [data set]. Zenodo. https://doi.org/10.5281/zenodo.3762278.
Hawco, N.J., Saito, M.A., 2018. Competitive inhibition of cobalt uptake by zinc and manganese in a pacific Prochlorococcus strain: insights into metal homeostasis in a streamlined oligotrophic cyanobacterium. Limnol. Oceanogr. 63 (5), 2229–2249.
Ho, T.Y., 2013. Nickel limitation of nitrogen fixation in Trichodesmium. Limnol. Oceanogr. 58 (1), 112–120.
Horner, T.J., Lee, R.B., Henderson, G.M., Rickaby, R.E., 2013. Nonspecific uptake and homeostasis drive the oceanic cadmium cycle. Proc. Nat. Acad. Sci. 110 (7), 2500–2505.
Hudson, R.J., Morel, F.M., 1993. Trace metal transport by marine microorganisms: implications of metal coordination kinetics. Deep-Sea Res. I Oceanogr. Res. Pap. 40 (1), 129–150.
Huertas, M.J., López-Maury, L., Giner-Lamia, J., Sánchez-Riego, A.M., Florencio, F.J., 2014. Metals in cyanobacteria: analysis of the copper, nickel, cobalt and arsenic homeostasis mechanisms. Life 4 (4), 865–886.
Irving, H.M.N.H., Williams, R., 1953. 637. The stability of transition-metal complexes. Journal of the Chemical Society (Resumed) 3192–3210.
Jacquot, J.E., Moffett, J.W., 2015. Copper distribution and speciation across the International GEOTRACES Section GA03. Deep-Sea Res. II Top. Stud. Oceanogr. 116, 187–207.
John, S.G., Conway, T.M., 2014. A role for scavenging in the marine biogeochemical cycling of zinc and zinc isotopes. Earth Planet. Sci. Lett. 394, 159–167.
John, S.G., Geis, R.W., Saito, M.A., Boyle, E.A., 2007. Zinc isotope fractionation during high-affinity and low-affinity zinc transport by the marine diatom *Thalassiosira oceanica*. Limnol. Oceanogr. 52 (6), 2710–2714.
Klakl, E., Korkisch, J., 1969. Anion-exchange behaviour of several elements in hydrobromic acid-organic solvent media. Talanta 16 (8), 1177–1190.
Korkisch, J., Hazan, I., 1965. Anion exchange separations in hydrobromic acid-organic solvent media. Anal. Chem. 37 (6), 707–710.
Little, S.H., Vance, D., Walker-Brown, C., Landing, W.M., 2014. The oceanic mass balance of copper and zinc isotopes, investigated by analysis of their inputs, and outputs to ferromanganese oxide sediments. Geochim. Cosmochim. Acta 125, 673–693.
Little, S.H., Vance, D., McManus, J., Severmann, S., Lyons, T.W., 2017. Copper isotope signatures in modern marine sediments. Geochim. Cosmochim. Acta 212, 253–273.
Lacan, F., Francois, R., Ji, Y., Sherrell, R.M., 2006. Cadmium isotopic composition in the ocean. Geochimica et cosmochimica acta 70 (20), 5104–5118.
Little, S.H., Archer, C., Milne, A., Schlosser, C., Achterberg, E.P., Lohan, M.C., Vance, D., 2018. Paired dissolved and particulate phase Cu isotope distributions in the South Atlantic. Chem. Geol. 502, 29–43.
Macomber, L., Imlay, J.A., 2009. The iron-sulfur clusters of dehydratases are primary intracellular targets of copper toxicity. Proc. Natl. Acad. Sci. 106 (20), 8344–8349.
Moore, C.M., Mills, M.M., Arrigo, K.R., Berman-Frank, I., Bopp, L., Boyd, P.W., Galbraith, E.D., Geider, R.J., Guieu, C., Jaccard, S.L., Jickells, T.D., La Roche, J., Lenton, T.M., Mahowald, N.M., Marañón, E., Marinov, I., Morre, J.K., Nakatsuka, T., Oschlies, A., Saito, M.A., Thingstad, T.F., Tsuda, A., Ulloa, O., 2013. Processes and patterns of oceanic nutrient limitation. Nat. Geosci. 6 (9), 701–710.
Moynier, F., Vance, D., Fujii, T., Savage, P., 2017. The isotope geochemistry of zinc and copper. Rev. Mineral. Geochem. 82 (1), 543–600.
Nelson, F., Rush, R.M., Kraus, K.A., 1960. Anion-exchange studies. XXVII. Adsorbability of a number of elements in HCl-HF solutions. J. Am. Chem. Soc. 82 (2), 339–348.
Posacka, A.M., Semeniuk, D.M., Whitby, H., van den Berg, C.M., Cullen, J.T., Orians, K., Maldonado, M.T., 2017. Dissolved copper (dCu) biogeochemical cycling in the subarctic Northeast Pacific and a call for improving methodologies. Mar. Chem. 196, 47–61.
Price, N.M., Morel, F.M., 1991. Colimitation of phytoplankton growth by nickel and nitrogen. Limnol. Oceanogr. 36 (6), 1071–1077.
Ratié, G., Jouvin, D., Garnier, J., Rouxel, O., Miska, S., Guimaraes, E., Cruz Vieira, L., Sivry, Y., Zelano, I., Montarges-Pelletier, E., Thil, F., Quantin, C., 2015. Nickel isotope fractionation during tropical weathering of ultramafic rocks. Chem. Geol. 402, 68–76.
Ripperger, S., Rehkämper, M., Porcelli, D., Halliday, A.N., 2007. Cadmium isotope fractionation in seawater—a signature of biological activity. Earth Planet. Sci. Lett. 261 (3–4), 670–684.
Rodriguez, I.B., Ho, T.Y., 2014. Diel nitrogen fixation pattern of Trichodesmium: the interactive control of light and Ni. Sci. Rep. 4, 4445.
Rue, E.L., Bruland, K.W., 1995. Complexation of iron (III) by natural organic ligands in the Central North Pacific as determined by a new competitive ligand equilibration/adsorptive cathodic stripping voltammetric method. Mar. Chem. 50 (1–4), 117–138.
Saito, M.A., Moffett, J.W., DiTullio, G.R., 2004. Cobalt and nickel in the Peru upwelling region: a major flux of labile cobalt utilized as a micronutrient. Glob. Biogeochem. Cycles 18 (4) Dec.
Saito, M.A., Rocap, G., Moffett, J.W., 2005. Production of cobalt binding ligands in a Synechococcus feature at the Costa Rica upwelling dome. Limnol. Oceanogr. 50 (1), 279–290.
Samanta, M., Ellwood, M.J., Strzepek, R.F., 2018. Zinc isotope fractionation by *Emiliania huxleyi* cultured across a range of free zinc ion concentrations. Limnol. Oceanogr. 63 (2), 660–671.
Semeniuk, D.M., Bundy, R.M., Payne, C.D., Barbeau, K.A., Maldonado, M.T., 2015. Acquisition of organically complexed copper by marine phytoplankton and bacteria in the northeast subarctic Pacific Ocean. Mar. Chem. 173, 222–233.
Sunda, W.G., Huntsman, S.A., 1998. Interactive effects of external manganese, the toxic metals copper and zinc, and light in controlling cellular manganese and growth in a coastal diatom. Limnol. Oceanogr. 43 (7), 1467–1475.
Takano, S., Tanimizu, M., Hirata, T., Sohrin, Y., 2014. Isotopic constraints on biogeochemical cycling of copper in the ocean. Nat. Commun. 5, 5663.
Takano, S., Tanimizu, M., Hirata, T., Shin, K.C., Fukami, Y., Suzuki, K., Sohrin, Y., 2017. A simple and rapid method for isotopic analysis of nickel, copper, and zinc in seawater using chelating extraction and anion exchange. Anal. Chim. Acta 967, 1–11.
Takano, S., Liao, W.H., Tian, H.A., Huang, K.F., Ho, T.Y., Sohrin, Y., 2020. Sources of particulate Ni and Cu in the water column of the northern South China Sea: evidence from elemental and isotope ratios in aerosols and sinking particles. Mar. Chem. 219, 103751.
Thompson, C.M., Ellwood, M.J., 2014. Dissolved copper isotope biogeochemistry in the Tasman Sea, SW Pacific Ocean. Mar. Chem. 165, 1–9.
Twining, B.S., Baines, S.B., Vogt, S., Nelson, D.M., 2012. Role of diatoms in nickel biogeochemistry in the ocean. Glob. Biogeochem. Cycles 26 (4).
Vance, D., Archer, C., Bermin, J., Perkins, J., Statham, P.J., Lohan, M.C., Ellwood, M.J., Mills, R.A., 2008. The copper isotope geochemistry of rivers and the oceans. Earth Planet. Sci. Lett. 274 (1–2), 204–213.
Vance, D., Little, S.H., Archer, C., Cameron, V., Andersen, M.B., Rijkenberg, M.J., Lyons, T.W., 2016. The oceanic budgets of nickel and zinc isotopes: the importance of sulfidic environments as illustrated by the Black Sea. Philos. Trans. R. Soc. A Math. Phys. Eng. Sci. 374 (2081), 20150294.
Waldron, K.J., Robinson, N.J., 2009. How do bacterial cells ensure that metalloproteins get the correct metal? Nature Review Microbiology 7 (1), 25–35.
Wang, R.M., Archer, C., Bowie, A.R., Vance, D., 2019. Zinc and nickel isotopes in seawater from the Indian Sector of the Southern Ocean: the impact of natural iron fertilization versus Southern Ocean hydrography and biogeochemistry. Chem. Geol. 511, 452–464.
Whitby, H., Posacka, A.M., Maldonado, M.T., van den Berg, C.M., 2018. Copper-binding ligands in the NE Pacific. Mar. Chem. 204, 36–48.
Yang, S.C., Welter, L., Kolatkar, A., Nieva, J., Waitman, K.R., Huang, K.F., Liao, W.H., Takano, S., Berelson, W.M., West, A.J., Kuhn, P., John, S.G., 2019. A new anion exchange purification method for Cu stable isotopes in blood samples. Anal. Bioanal. Chem. 411 (3), 765–776.